Passive remediation of mine waters from Parys Mountain (Wales): Laboratory column experiments

Ricardo Millán-Becerro [a],[*], Carlos R. Cánovas [a], Francisco Macías [a], Tobias S. Roetting [b], Louise Siddorn [c], Peter Stanley [c], José Miguel Nieto [a]

[a] Department of Earth Sciences & Research Center on Natural Resources, Health and the Environment, University of Huelva, 21071, Huelva, Spain
[b] WSP UK Ltd, 70 Chancery Lane, London, WC2A 1AF, UK
[c] Natural Resources Wales, Tŷ Cambria, 29 Newport Road, Cardiff, CF24 0TP, Wales, UK

ARTICLE INFO

ABSTRACT

This study evaluates the effectiveness of dispersed alkaline substrate (DAS) technology to treat highly acidic and contaminated leachates from the oxidation of sulfide-rich mining wastes under wet temperate oceanic climate conditions. To address this issue, leachates from the abandoned mine at Parys Mountain (NW Wales) were passed through two sets of multistep columns filled with a mixture of a fine-grained alkaline reagent (i.e., limestone, MgO, or $BaCO_3$) scattered in an inert matrix. The set of columns with the limestone-DAS plus MgO-DAS combination achieved a near total removal of Fe, Al, Zn, Cu, Mn, As, Co, Cd, and Ni. However, the elimination of SO_4 was not significant (around 7%). The limestone-DAS plus $BaCO_3$-DAS combination also achieved a high effectiveness for base metal/loids, allowing the removal of Fe, Al, Zn, Cu, As, and Cd with rates of nearly 100%. In addition, the system with the $BaCO_3$-step had a higher effectiveness in eliminating SO_4 (around 53%) than the combined treatment with the MgO-step. According to PHREEQC code calculations, the precipitation of oxy-hydroxy-sulfates (i.e., schwertmannite and basaluminite) and carbonate (i.e., malachite, hydrozincite and calcite) phases may have controlled the solubility of pollutants during the passive treatment. The chemical compositions of the treated waters complied with the threshold values defined by irrigation standards, except for Mn in the $BaCO_3$-DAS output.

1. Introduction

The oxidation of sulfide-rich wastes from mining activity generates acidic waters with high dissolved concentrations of sulfate and metal/loids (e.g., Fe, Al, Zn, Cu, As, and Cd). These highly polluted waters, known as acid mine drainage (AMD), often flow from abandoned mining districts to reservoirs and rivers and can even reach the oceans depending on their proximity to these or pollution intensity (Dean et al., 2013; Nieto et al., 2013; Cánovas et al., 2016). Indeed, AMD may deteriorate the chemical quality of water bodies, causing adverse effects on aquatic organisms and limiting their use for human consumption, in agriculture, and industry (Akcil and Koldas, 2006; Tripole et al., 2006). Some of the locations most affected by AMD occur in the United States, where around 500,000 abandoned mines are affecting 25,000 km of streams with AMD (DeGraff, 2007). The Odiel and Tinto River basins

(Iberian Pyrite Belt [IPB], SW Iberian Peninsula) are other examples of highly degraded areas due to past intense mining activity. Here, there are around thirty abandoned mines that discharge AMD into both river basins (Sarmiento et al., 2009), resulting in around 460 km of extremely polluted watercourses (Sarmiento et al., 2009; Cánovas et al., 2016). These rivers annually discharge thousands of tonnes of metal/loids to the Ría de Huelva estuary that subsequently enter the Atlantic Ocean (Nieto et al., 2013). The UK also has a significant legacy of metal-rich sulfide wastes deriving from around 4900 abandoned mines in, which oxidation generates AMD causing great environmental concern (Mayes et al., 2010). The abandoned mines on Parys Mountain (originally named Mynydd Trysglwyn) located in Anglesey (NW Wales) are one of these pollution sources, which contribute around 34–71% of the total Fe and Cu released from abandoned mining districts nationwide (Mayes et al., 2010). According to Chalkley et al. (2019), the highly acidic and

polluted AMD from Parys Mountain is discharged into freshwater bodies, ending up in the Irish Sea, being an important route for coastal and marine pollution. These authors highlighted the need to minimize pollution from Parys Mountain into the Irish Sea, as it has negative effects on the marine biota of the area. The adoption of remediation measures is therefore crucial to achieve this goal.

Mine waters can be remediated by active or passive technologies (Johnson and Hallberg, 2005). Active treatments are usually employed in operating mines due to the need for remediating large volumes of water. However, these treatments require the continuous use of electrical energy and continuous addition of chemical reagents, as well as intensive maintenance, monitoring, and management of the wastes. Therefore, active treatments are commonly unsuitable for abandoned mines sites. On the contrary, passive technologies are more appropriate than active treatments in abandoned mines since they do not require energy consumption, the continuous provision of chemicals, or regular maintenance (Johnson and Hallberg, 2005). Most AMD contamination derives from derelict or abandoned mines that were previously exploited by mining companies which are now exempt of legal responsibility and are thus typically considered orphan sites. Some sites such as Parys Mountain have been sporadically exploited during the Bronze Age and Roman times and from the 18th to 20th century (Bevins et al., 2010). Considering the longevity of AMD generation processes, estimated at several hundred years (Younger, 1997), passive treatment technologies are the most suitable for the remediation of AMD from abandoned mining districts (Johnson and Hallberg, 2005). Currently, dispersed alkaline substrate (DAS) technology is considered the most suitable passive option to treat highly contaminated AMD waters due to environmental and economic criteria (Ayora et al., 2013; Orden et al., 2021). DAS technology involves the use of a mixture of a fine-grained alkaline reagent (commonly limestone ($CaCO_3$) and magnesia (MgO)) with an inert matrix of large surface area (usually wood chips) to avoid the passivation and clogging problems associated with the precipitation of Fe and Al mineral phases (Macías et al., 2012b; Ayora et al., 2013). Despite their high effectiveness in neutralizing the acidity of AMD and removing dissolved metal/loids, conventional reagents (i.e., $CaCO_3$ and MgO) are unable to effectively eliminate sulfate from these highly acidic and polluted leachates. To achieve this, Torres et al. (2018) used witherite ($BaCO_3$) as an alkaline reagent in the DAS treatment of AMD, achieving high removal rates of sulfate, as well as for other contaminants commonly removed by conventional reagents. DAS technology was initially designed and later optimized for the treatment of AMD waters from the IPB under dry Mediterranean climate conditions (Rötting et al., 2006a, 2006b; Caraballo et al., 2009, 2011a; Macías et al., 2012b; Ayora et al., 2013; Torres et al., 2018). Additionally, the use of this passive treatment technology has been extended to other world regions such as Ecuador and Canada, with dry-megathermic and cold climate conditions, respectively (Rakotonimaro et al., 2016, 2018; Delgado et al., 2019). Elements dissolved in natural waters are released through weathering processes and their transport through the hydrologic cycle is facilitated by microbial processes (Nordstrom, 2011), especially in AMD environments. All these processes are strongly controlled by climate conditions. Thus, pronounced droughts in AMD sites may lead to the formation soluble salts on the surface of mine wastes and soils, which will be redissolved giving rise to elevated sulfate and metal concentrations. On the other hand, in regions governed by high levels of rainfall, meteoric waters may cause a decrease in contaminant levels but an increase in flows. The effectiveness of passive treatment systems such as DAS technology in different regions worldwide will depend on these fluctuations in water composition and flows related to different climate conditions. However, the effectiveness of DAS technology has not been previously tested for AMD from mining districts within a wet temperate oceanic climate. To bridge this gap in knowledge, this work aims to assess the potential application of a multistep DAS system to remediate AMD from the abandoned Parys Mountain mines, one of the most polluting mine complexes in Wales, UK (Mayes et al., 2010). Thus, two

sets of sequential treatments (i.e., limestone-DAS with MgO-DAS or $BaCO_3$-DAS) were tested to discern the most appropriate combination to use at mine sites with the abovementioned climatic conditions.

2. Materials and methods

2.1. Study site

The study area includes the abandoned mines at Parys Mountain, located in Anglesey, NW Wales (Fig. 1), an area widely known for copper mining. Copper ore extraction commenced in the mid-18th century, with Parys Mountain initially being exploited as two separate mines. The first at the Cerrig y Bleiddia Farm in 1761, later becoming the Mona mine, and the second on land at the neighbouring Parys Farm (Parys Mine) in 1770 (Rowlands, 1981). These mines were operated with extraction through two great opencasts working the orebody known as the "Great Lode", also referred to as the "Opencast Lode" (Bevins et al., 2010), and by using scrap from precipitation ponds from as early as 1772 (Rowlands, 1981). By the end of the 18th century, Parys Mountain had become the largest producer of copper in the world. Bevins et al. (2010) discussed the provenance of the deposits and their, pre- and post-mining mineralogy, noting that the Great Lode originally had a gossan cap, which hosted abundant anglesite. Production had tailed off by the 1850's and copper ore extraction through underground mining continued until c.1880 when the mine was formally abandoned. Mining of Pb-Zn bluestone deposits continued with a third mine, Morfa-du, opening on the extreme western end of the mountain. From 1882 to 1911, the Mona and Morfa-du mines generated 5259 tonnes of Pb and Zn (Dewey and Smith, 1922). The extraction of copper from precipitation ponds continued until the 1950's (Bevins et al., 2010) when the valves of a choke dam near the Garth Daniel Shaft on the Joint Adit Level/Dyffryn Adda adit were closed.

The Parys Mountain deposit is a volcanic-hosted massive sulfide deposit consisting of lenses of massive Zn-Pb-Cu sulfides at and near the contact between Ordovician shales and overlying Lower Silurian rhyolites (Barrett et al., 2001). Cu-bearing stockwork veins are located in the upper part of the Ordovician shales and Cu-bearing massive mineralization occurs in the Lower Silurian shales (Barrett et al., 2001).

Historical mining activities at the Parys Mountain deposit have resulted in the accumulation of important amounts of metal-rich wastes with a high AMD generation capacity (Ríos et al., 2008; Younger and Potter, 2012; Crane et al., 2017). The continuous discharge of this acidic and metal-rich water from the mine adits and spoil heaps is transported to the Irish Sea via the Afon Goch Amlwch River in the north and the Afon Goch Dulas River in the south, resulting in a significant outflow of Fe, Cu, Cd, and Zn (Mayes et al., 2010). A large acidic lake of mine water had accumulated within Parys Mountain stimulating flooding concern in the town of Amlwch. Intervention work commenced by the Anglesey County Council and supported by the predecessor body of Natural Resources Wales (NRW) in 2002 removed the Garth Daniel Shaft choke dam introducing the primary Parys Mountain drainage route via the Dyffryn Adda adit to the Afon Goch Amlwch. The Morfa-du adit has a separate small loading in comparison. Seasonal contamination has now been recorded in the NRW monitoring of the Afon Goch Dulas to the south.

2.2. Experimental design

Two multistep DAS systems were built in the laboratory to treat the AMD (Fig. 2). Each DAS system consisted of three polymethyl methacrylate columns (40 cm in height and 6 cm in diameter) each filled with 20 cm of DAS reagent material (80% (v/v) wood chips, 20% (v/v) alkaline reactive) and a 3 cm layer of glass pearls (3 mm diameter) at the bottom to favor water drainage. Two columns were filled with limestone-DAS (Cc-DAS1 and Cc-DAS2) and the third with MgO-DAS (system 1) or $BaCO_3$-DAS (system 2). According to Caraballo et al.
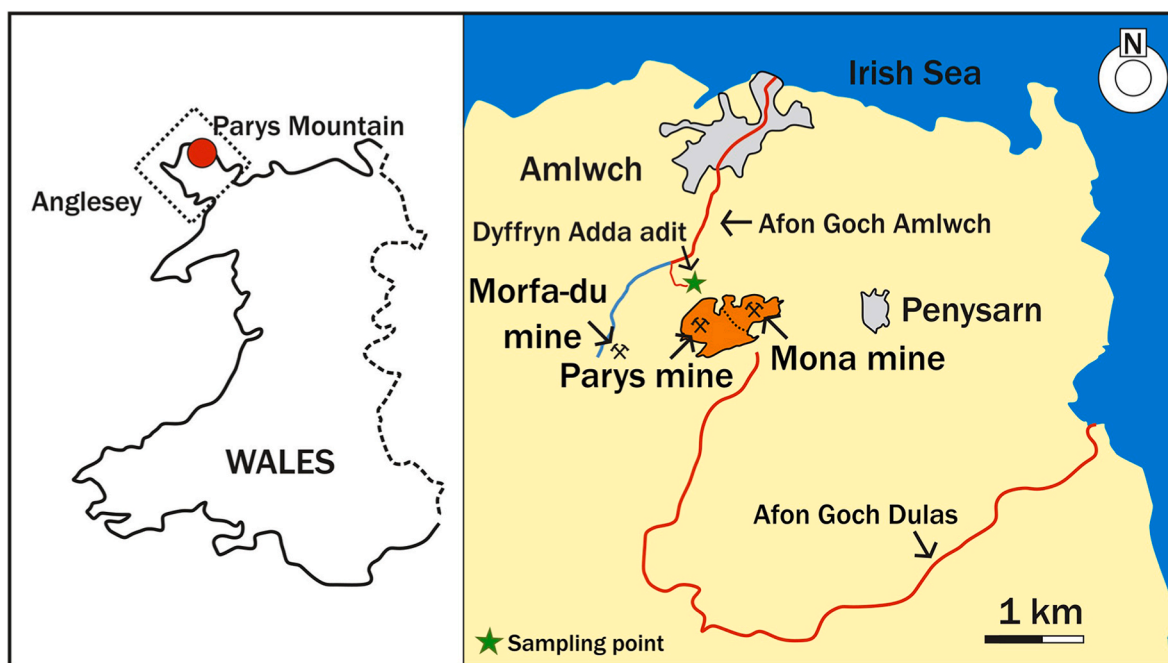
Fig. 1. Location map of the abandoned mines at Parys Mountain in Anglesey, NW Wales.
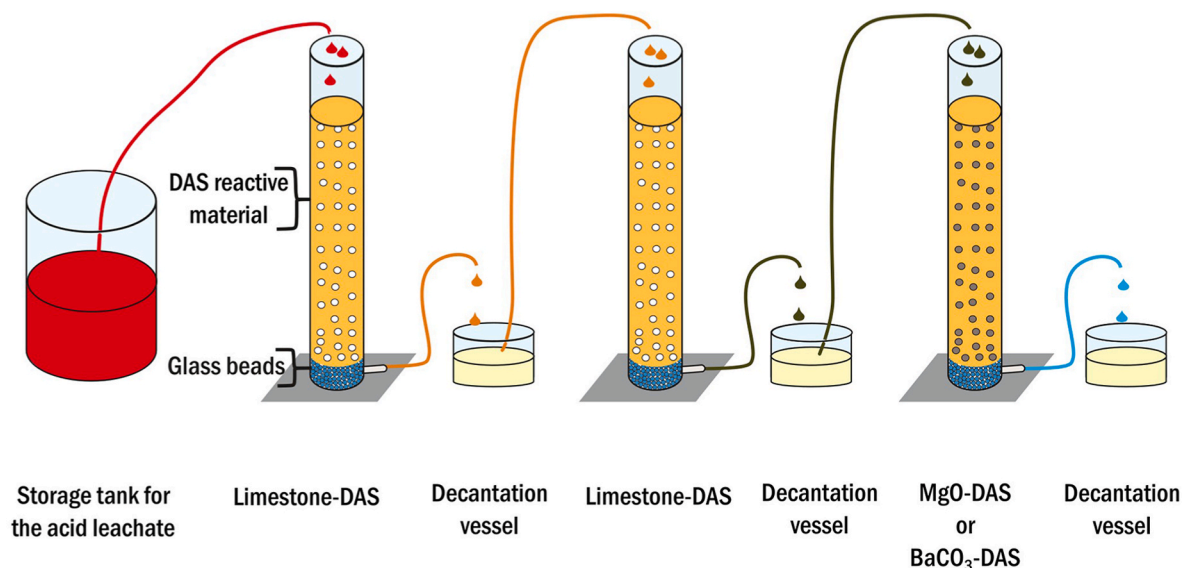

Fig. 2. Schematic setup of the limestone-DAS + MgO-DAS (System 1) and limestone-DAS + BaCO$_3$-DAS (System 2) laboratory columns.

(2011b), the high porosity of the DAS mixture is essential to maintain hydraulic conductivity and retard clogging problems suffered by passive treatment systems due to the precipitation of solids within the pore spaces of the reactive material. In addition, each column was connected to a decantation vessel (DV) (7 cm in height and 9 cm in diameter) with a capacity of 445 cm^3 to favor the sedimentation of newly-formed precipitates and to reach equilibrium with the atmosphere. A 25-L storage tank was used as an AMD water source and as an iron oxidation step prior to the reactive columns. This tank simulated a Natural Fe-Oxidizing Lagoon (NFOL), a step preceding the DAS treatments, which is intended to oxidize and partially eliminate the Fe dissolved in

the AMD in order to improve the performance of DAS treatment systems (Macías et al., 2012a). The different components of the DAS systems were connected in series through plastic pipes. During each treatment, the AMD was pumped from the 25-L storage tank and conducted through the DAS systems by a peristaltic pump, with a constant flow rate of 0.3 ml/min, flowing from the top of the DAS columns downward through the reactive materials and out of the drain pipe into the decantation vessel. The multistep DAS treatment systems were run under optimal conditions for 21 weeks, allowing the successful treatment of around 64 L of acid leachates each.

The reactive materials used in these laboratory experiments were

magnesium limestone (99% calcite ($CaCO_3$)) purchased at a local quarry (grain size 0.063–1 mm), magnesia powder (70% periclase (MgO)) supplied by Magnesitas de Navarra S.A., and barium carbonate powder (99% witherite ($BaCO_3$)) provided by Mario Pilato Blat S.A. The leachate used in the column experiments was collected from the Dyffryn Adda adit (Fig. 1), which discharges AMD to the Afon Goch Amlwch with a flow of 12 L/s.

The main physical characteristics of the different DAS columns can be seen in Table S1. The residence times of AMD waters in the columns, calculated from the porosity and the input water flow, were around 26–28 h depending on the DAS reactive material (Table S1).

2.3. Water sampling and analysis

Water samples were obtained every week from the different steps of each DAS treatment system; input solution, column outputs, and decantation vessels. Different physical-chemical parameters such as pH, electrical conductivity (EC), redox potential (ORP), and temperature were determined in situ using a CRISON multi-parameter portable equipment MM 40+, previously calibrated with buffer solutions of 4.01, 7.00, and 9.21 for pH and with standard solutions of 147 μS/cm, 1413 μS/cm, and 12.88 mS/cm for EC. In the case of ORP, the accuracy of the measurements was verified using standard solutions (i.e., 220 and 470 mV). The ORP measurements were corrected according to Nordstrom and Wilde (1998) to obtain standard hydrogen electrode Eh values. Alkalinity (Alk) was measured by CHEMetrics® Total Titrets®, with a range of 10–100 or 100–1000 mg/L as $CaCO_3$ equivalents.

The sampled solutions were filtered at 0.22 μm with Teflon filters, acidified to pH < 1 with ultrapure HNO_3 (2%), and subsequently stored at 4 °C until their chemical analysis. The major element (Al, Ca, Cu, Fe, Mg, Mn, S, and Zn) concentrations were determined by atomic emission spectroscopy with inductively coupled plasma (ICP-AES, Jobin Yvon Ultima 2) while the trace element (As, Ba, Cd, Co, and Ni) contents were analyzed by mass spectrometry with inductively coupled plasma (ICP-MS; Agilent 7700). All analyses were performed in the Central R + D Laboratories of the University of Huelva, Spain. The detection limits were: 0.2 mg/L for S; 0.05 mg/L for Fe and Mg, 0.02 mg/L for Al, Cu, Ca, Mn, and Zn; and 0.1 μg/L for the trace elements. In the laboratory, home-made standards with concentrations within the range of the leachate samples were used to control the quality of the analyses. Blank solutions made with the same matrix as the samples were included in each analysis sequence. Furthermore, dilutions (from 1:10 to 1:200) were carried out to ensure that the sample concentrations were within the concentration range of the standards. The average measurement error was below 5% for all samples. The determination of Fe(II) and total Fe contents was conducted by colorimetry at 510 nm using a Hach DR/890 colorimeter. The limit of detection was 0.3 mg/L and the measurement error was better than 5%. Ferric iron (Fe(III)) contents were calculated as the difference between total Fe and Fe(II).

The saturation indices (SI) of the water samples with respect to certain mineral phases controlling the solubility of pollutants during the DAS treatments were obtained using the PHREEQC 3.0 geochemical code (Parkhurst and Appelo, 2005) with the WATEQ4f thermodynamic database (Allison et al., 1991), amended to add the thermodynamic data of schwertmannite (ideal reaction: $Fe_8O_8(SO_4)_{1.5}(OH)_5 + 21H^+ = 8Fe^{+3} + 13H_2O + 1.5SO_4^{-2}$; $logK_{sp}$: 18.8) from Sánchez-España et al. (2011) and hydrozincite (ideal reaction: $Zn_5(CO_3)_2(OH)_6 + 6H^+ = 5Zn^{+2} + 2CO_3^{-2} + 6H_2O$; $logK_{sp}$: 9.69) from Schindler et al. (1969).

3. Results and discussion

3.1. Hydrochemistry of DAS treatment systems

To understand the performance of the different components of the multistep DAS systems described in this study, this section will present the average spatial evolution of the physicochemical parameters (i.e.,

pH, EC, ORP, and alkalinity), as well as the behavior of the main pollutants dissolved in the AMD waters (Fig. 3).

The results of the different treatments are shown in Tables S2 and S3. The AMD used in this study exhibited average pH, EC, and ORP values of 2.30, 3.01 mS/cm, and 538 mV, respectively, alongside a net acidity of 1400 mg/L as $CaCO_3$ equivalents according to the definition of Kirby and Cravotta (2005), and high dissolved concentrations of pollutants, such as 2284 mg/L SO_4, 403 mg/L Fe, 57 mg/L Al, 54 mg/L Zn, 31 mg/L Cu, 12 mg/L Mn; as well as other minor elements, e.g., 360 μg/L As, 251 μg/L Co, 118 μg/L Cd and 111 μg/L Ni, among others (Fig. 3). In the starting AMD sample from Parys Mountain, around 26% of total Fe was as Fe(II). However, this Fe was oxidized to Fe(III) in the storage tank (Tables S2 and S3).

The calcite dissolution in the first limestone-DAS column (Cc-DAS 1) raised the pH of the acid leachate up to average values of 6.0. On the contrary, the ORP suffered a strong drop (from 538 to 257 mV), while the EC hardly decreased (from 3.01 to 2.92 mS/cm) (Fig. 3a,d). The significant decrease in the ORP value observed at the output column could have been due to the generation of partial reducing conditions within the reactive column by the presence of labile organic matter in the wood chips. The dissolution of the alkaline reagent caused an increase in alkalinity (from 0 to 89 mg/L as $CaCO_3$ equivalents) and in Ca and Mg concentrations (from 45 to 329 mg/L and from 70 to 240 mg/L, respectively). These changes in the AMD chemistry promoted the total elimination of Fe, Al, and As (Fig. 3b,c,e,f). Additionally, the SO_4 and Cu concentrations in the first limestone-DAS decreased from 2284 to 2134 mg/L (7% removal) and from 31 to 15 mg/L (50% elimination), respectively (Fig. 3b,c,e,f). The strong decrease in Fe and Al concentrations may have resulted from the precipitation of oxy-hydroxy-sulfates such as schwertmannite ($Fe_8O_8(OH)_5(SO_4)_{1.5} \bullet nH_2O$) and basaluminite ($Al_4(OH)_{10}SO_4 \bullet 5H_2O$) as predicted by the PHREEQC code (Fig. 4). These mineral phases could also have controlled the solubility of other contaminants, such as Cu and As, through co-precipitation and/or adsorption processes (Caraballo et al., 2011b). In addition, the decrease in Cu concentrations may have been associated to the precipitation of malachite ($Cu_3(CO_3)(OH)_2$), which was oversaturated according to PHREEQC (Fig. 4). Then, the water flowed into a decantation vessel (DV1), where a slight increase in the water pH (from 6.0 to 6.2) was noted, probably caused by the degassing of the CO_2 dissolved in the treated water upon its contact with the air. In this step, there was also a decrease in Cu concentrations from 15 to 7.0 mg/L; remaining dissolved 23% of the initial Cu concentration. In the second limestone-DAS column (Cc-DAS 2) and its decantation vessel (DV2), the treated waters showed pH values of up to around 6.7 and 6.8, respectively. After these steps, the ORP values decreased slightly (from 262 to 226 mV), while the EC values remained almost constant (Fig. 3a,d). The increase in the pH of the leachate was due to the same processes described above for Cc-DAS 1 and DV1, that is, the dissolution of carbonate materials in the column and degassing processes in the decantation vessel. The additional rise in pH allowed a significant reduction of the dissolved Cu concentrations (from 7.0 to 0.1 mg/L), as well as a slight decrease in Zn concentrations (from 53 to 48 mg/L) (Fig. 3c,f), which could be attributed to the precipitation of carbonate mineral phases (i.e., malachite and hydrozincite ($Zn_5(CO_3)_2(OH)_6$)) that were oversaturated in the output solutions derived from the second limestone-DAS (Fig. 4). The precipitation of newly-formed carbonates may have led to the decrease in alkalinity that took place in the second limestone-DAS (from 75 to 66 mg/L as $CaCO_3$ equivalents) (Fig. 3a,d). Of note, the concentrations of other divalent metals such as Mn, Co, Cd, and Ni remained nearly constant during the limestone-DAS treatment (Fig. 3c,f). This could be explained because the dissolution of calcite raised the leachate pH to values close to 7, which is insufficient to reduce the solubility of these metals since the precipitation of hydroxides of divalent metals commonly requires higher pH values (Cortina et al., 2003; Caraballo et al., 2010). Thus, other alkaline reagents capable of raising the leachate pH to values above 8.5 would be required (Cortina et al., 2003).
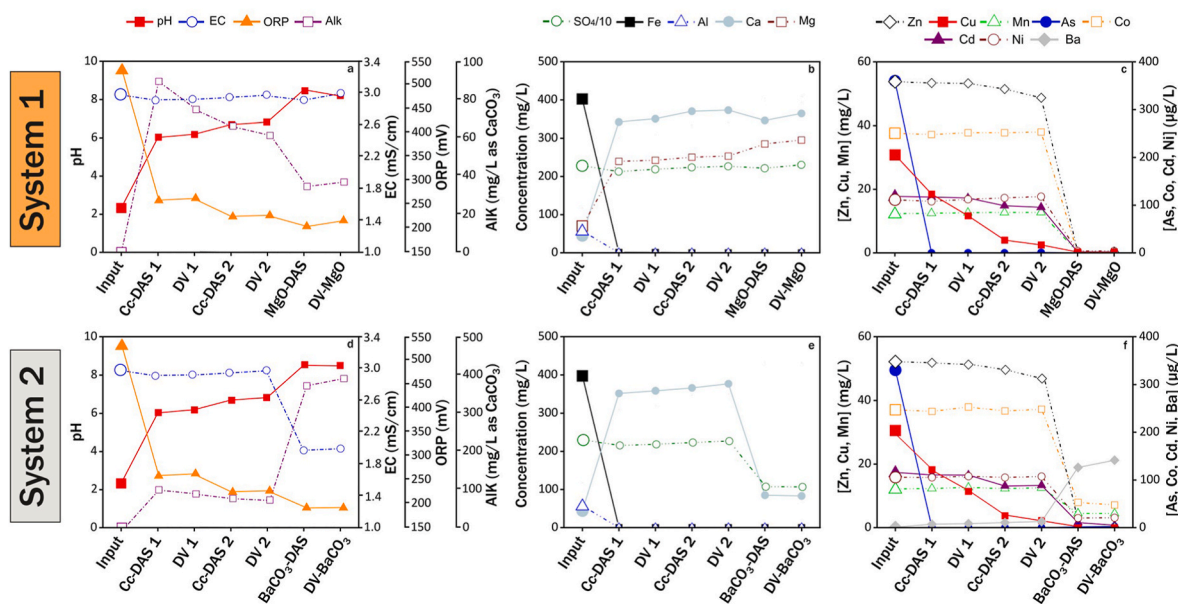
Fig. 3. Evolution in the physicochemical parameters and concentration of pollutants, along the different points of the multistep treatment systems; i.e., limestone-DAS + MgO-DAS (System 1) and limestone-DAS + BaCO$_3$-DAS (System 2).
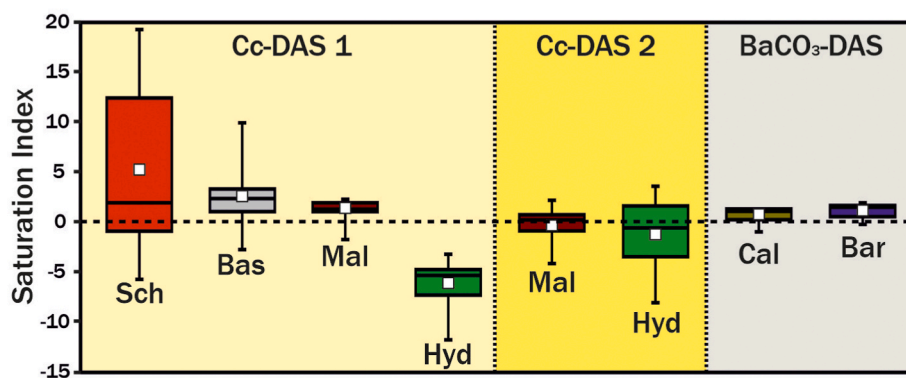

Fig. 4. Box and whisker diagrams showing saturation indices (SI) of the oversaturated mineral phases calculated according to PHREEQC code for the solutions from the reactive columns (i.e., limestone-DAS, MgO-DAS, and BaCO$_3$-DAS). Sch: schwertmannite, Bas: basaluminite, Mal: malachite, Hyd: hydrozincite, Cal: calcite, Bar: barite.

The inflowing solution in the MgO-DAS yielded pH values of around 6.8 and following its interaction with magnesium oxide, this value increased to approximately 8.5 (Fig. 3a). On the contrary, the ORP and EC values remained nearly constant (Fig. 3a). The rise in pH achieved the near total elimination of Zn, Mn, Co, Cd and Ni from solution (Fig. 3c). Here, the oversaturation of divalent metal mineral phases in the output waters from the MgO-DAS treatment had not been predicted by PHREEQC. However, Pérez-López et al. (2011) experimentally reported the precipitation of carbonate mineral phases (mainly hydrozincite as well as a lesser amount of loseyite ((Mn,Zn)$_7$(CO$_3$)$_2$(OH)$_{10}$)) as sinks of Zn, Mn, Co, and Ni in the AMD treatment with MgO-DAS. The decrease in dissolved Cd concentration during the treatment correlated perfectly with a reduction of the concentration of the aforementioned divalent metals, with squared correlation coefficients (R^2) between 0.95 and 0.99. Cd co-precipitation and/or adsorption with Zn and Mn carbonates (i.e., hydrozincite and loseyite) could therefore not be ruled out. The SO$_4$ concentration remained constant during the treatment of AMD leachates with MgO-DAS. Here, PHREEQC predicted an undersaturation of the solutions resulting from this treatment with respect to sulfate minerals.

In the BaCO$_3$-DAS treatment, an increase in pH (from 6.8 to 8.7) of the almost neutral pretreated water took place due to the dissolution of the alkaline reagent. After this step, The ORP values were almost constant, while the EC values dropped significantly (from 2.98 to 1.99 mS/cm) (Fig. 3d). The sharp pH increase promoted a significant decrease in the concentration of divalent metals such as Zn (from 48 to 1.3 mg/L), Mn (12–4.5 mg/L), Co (238-48 µg/L), Cd (118–5.2 µg/L), and Ni (107-20 µg/L) (Fig. 3f) due to mineral precipitation processes. In addition, the treatment of AMD with BaCO$_3$-DAS also led to a significant decrease in the SO$_4$ concentration (from 2269 to 1073 mg/L), which seemed to be concomitant with the significant decrease in EC values achieved in this step of the second DAS treatment system (Fig. 3d and e). According to PHREEQC, these solutions were oversaturated with respect to barite (BaSO$_4$) (Fig. 4). This could have explained the higher SO$_4$ removal capacity observed in this BaCO$_3$-DAS treatment whereas with respect to the MgO-DAS system, no oversaturation of any sulfate mineral phases was found. Contrarily, the PHREEQC modeling did not predict any oversaturation of the BaCO$_3$-DAS waters with respect to divalent metal phases. According to Torres et al. (2018), the precipitation of calcite during the treatment of AMD with BaCO$_3$-DAS may have controlled the solubility of divalent metals (i.e., Zn, Mn, Co, Cd, and Ni) in solution through co-precipitation processes. This carbonate phase was

oversaturated in the output waters from the BaCO$_3$-DAS treatment according to the PHREEQC modeling (Fig. 4). In addition, a strong decrease in Ca concentrations (from 377 to 85 mg/L) was observed during the BaCO$_3$-DAS treatment (Fig. 3e), which was consistent with calcite precipitation. Therefore, this mineral phase could have behaved as a sink for divalent metals during the treatment.

Overall, a clear pattern of contaminant removal associated with different mineral phases was observed. Thus, the removal of contaminants (i.e., Fe, Al, As, Cu, and Zn) produced from the limestone-DAS was mainly due to the precipitation of oxy-hydroxy-sulfates (i.e., schwertmannite and basaluminite), as well as the occurrence of newly-formed carbonates (i.e., malachite and hydrozincite). The elimination of pollutants (i.e., Zn, Mn, Co, Cd, and Ni) in the MgO-DAS and BaCO$_3$-DAS treatments may however have been controlled by the precipitation of carbonate phases (i.e., hydrozincite, loseyite, and calcite). Additionally, the decrease in SO$_4$ concentrations observed in the BaCO$_3$-DAS treatment may have resulted from barite precipitation. For the optimal performance of the multistep DAS systems proposed in this manuscript, it is essential that the input solutions to the MgO-DAS and BaCO$_3$-DAS treatments would not contain Fe and/or Al, since the mineral precipitation of trivalent metals would result in a very fast coating of the MgO and BaCO$_3$ grains (passivation of the reagent) and a decrease in the hydraulic conductivity of the MgO-DAS and BaCO$_3$-DAS mixtures (Caraballo et al., 2010). During the experiments, no problems were observed in the hydraulics of the treatment systems, indicating that the pore spaces occupied by the newly-formed solids were offset by the dissolution of the reagent grains. Despite the good performance of the systems, they could be improved modifying certain properties (e.g., wood chips, water flow, etc.) related to the properties of these mine waters. On the other hand, the future effects of climate change may profoundly impact the mine water composition and this should be considered when developing remediation systems. Thus, it is expected the occurrence of long droughts and short but intense rainy periods. The flushing of mine sites during these short rainy events will cause larger sudden increases in contaminant concentrations with climate change and higher average concentrations will be observed during longer low-flow periods (Nordstrom, 2009). Therefore, these conditions should be considered when planning and implementing remediation systems in the near future.

3.2. Pollutant removal and water quality evaluation

The first multistep DAS system deployed (i.e., limestone-DAS + MgO-DAS) achieved removal percentages of 100% for Fe, Al, Zn, Cu, Mn, As, and Co, and around 98% of Cd and close to 96% for Ni (Fig. 3b and c). This multistep DAS system was not, however, effective for SO$_4$ removal. These results are similar to those achieved in the pilot DAS treatment plant built at the abandoned Monte Romero mine located in the IPB (Macías et al., 2012a, 2012b).

The second multistep treatment system (i.e., limestone-DAS + BaCO$_3$-DAS) caused the total elimination of the dissolved concentrations of Fe, Al, Cu, and As; in fact, their concentrations in solutions from the BaCO$_3$-DAS were close to or below the ICP-AES and ICP-MS detection limits. Additionally, a strong reduction in the concentration of divalent metals such as Zn, Cd, Co, and Ni took place, reaching average removal percentages of 81–97% (Fig. 3f). On the contrary, a lower performance was obtained for other potentially toxic pollutants such as SO$_4$ and Mn, which were scarcely removed during the treatment, reaching average percentages of 53–63%. The performance of the BaCO$_3$-DAS treatment for metal removal obtained in this work was similar to that reported by Torres et al. (2018). However, different performances between both BaCO$_3$-DAS treatments were observed for SO$_4$ (average elimination rates of 53 and 99%, respectively). This fact could be due to two main causes; on the one hand, the higher SO$_4$ load received by the BaCO$_3$-DAS treatment described in this work with respect to the treatment reported by Torres et al. (2018) (i.e., 1.0 and 0.7 g/day, respectively), and on the

other hand, the lower amount of alkaline reagent used in this research work compared to that reported by the aforementioned authors (i.e., 175 and 300 g of BaCO$_3$, respectively). As mentioned previously, the precipitation of barite (BaSO$_4$) may have controlled the solubility of SO$_4$ during the BaCO$_3$-DAS treatment (Fig. 4). In this study, the Ba/SO$_4$ molar ratio in the solutions from the BaCO$_3$-DAS treatment was $8.04*10^{-5}$, while this molar ratio in the solutions from the DAS treatment reported by Torres et al. (2018) was 0.54. This fact indicates a Ba deficiency in the AMD solutions treated by the BaCO$_3$-DAS proposed in this research. More studies are necessary to increase the effectiveness of the treatment with respect to SO$_4$.

A modified Ficklin diagram was constructed to assess the improvement in water quality achieved in the two multistep treatment systems described here (Fig. 5) This diagram is commonly used to categorize AMD waters according to their pH and metal concentration (Ficklin et al., 1992; Ríos et al., 2008). The categories range from high acidity (HA) to moderate alkalinity (MAlk) and from extreme metallic (EM) to low metallic (LM) according to the level of acidity and metals contained. As shown in Fig. 5, the AMD from Parys Mountain was classified as high acidity-extreme metallic (HA-EM). Once the AMD leachate flowed through the limestone-DAS treatment (Cc-DAS 1 and Cc-DAS2), the solutions reached the near neutral field but with a high metal content (NN-HM). After this step, the AMD waters flowed through an MgO-DAS or BaCO$_3$-DAS treatment, depending on the multistep system. The best chemical quality of the water was achieved through the MgO-DAS treatment. Thus, solutions from MgO-DAS were characterized by a low metal content and pH values close to neutrality (Fig. 5). When considering the BaCO$_3$-DAS treatment, most of the output solutions remained in the near neutral field with high concentrations of metals, but with an average metallic content of two orders of magnitude lower than those of the input solutions (Fig. 5).

The average concentrations of the main pollutants analyzed in the outputs of both multistep DAS treatment systems (i.e., limestone-DAS + MgO-DAS or BaCO$_3$-DAS) were compared with the threshold values for these elements in irrigation (FAO; Ayers and Westcot, 1985) and drinking waters (WHO, 2011) to check the quality improvement obtained through using the treatment systems (Table 1). The best chemical quality of the water was achieved through the MgO-DAS treatment. Thus, all the contaminants analyzed in the waters sampled from the
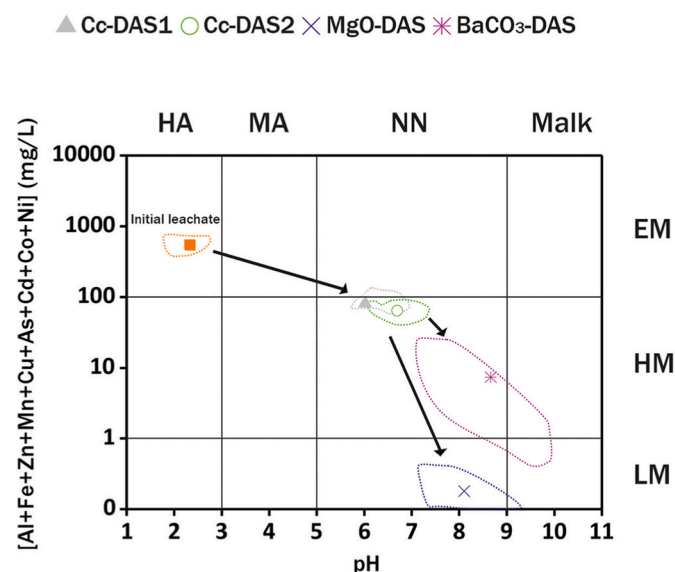

Fig. 5. Modified Ficklin diagram for the different DAS columns. HA: high acidity, MA: moderate acidity, NN: near neutral, Malk: moderate alkalinity, EM: extreme metallic, HM: high metallic, LM: low metallic. The symbols are the average values and the areas defined by dashed lines are the data corresponding to the 21 weeks of the experiment.

Table 1
Chemical composition of the initial acid leachate and the solutions sampled at the output of the multistep treatment systems; i.e., limestone-DAS + MgO-DAS (System 1) and limestone-DAS + BaCO₃-DAS (System 2) (average values of the 21 weeks of experiment), and comparison with the limit values established for metal and toxic element concentration in irrigation water and drinking water.

	Initial leachate	System 1 output	System 2 output	FAO	WHO
Major elements (mg/L)					
SO₄	2290	2311	1068	n.r.l.	250
Fe	400	<l.d.	<l.d.	5	5
Al	57.3	<l.d.	<l.d.	5	0.2
Zn	52.9	<l.d.	0.75	2	3
Cu	30.7	<l.d.	<l.d.	0.2	2
Mn	12.2	<l.d.	4.49	0.4	0.2
Minor elements (μg/L)					
As	360	<l.d.	<l.d.	100	10
Co	249	<l.d.	47.6	50	n.r.l.
Cd	117	2.03	4.71	10	3
Ni	109	4.08	20.8	200	70
Ba	2.63	16.7	141	n.r.l.	700

<l.d.: below detection limit, n.r.l.: no referenced limit.

MgO-DAS treatment output complied with the recommendations established by the FAO for irrigation waters. However, the waters from the BaCO₃-DAS system could not be used for irrigation because their Mn concentrations exceeded the thresholds determined by the FAO (Table 1). Notably both multistep systems yielded output solutions with Fe, Al, Zn, Cu, As, and Ni concentrations below the threshold levels established by the WHO. In addition, the output waters from the MgO-DAS treatment also fulfilled the WHO requirements for Mn and Cd (Table 1). However, the dissolved SO₄ concentrations in the solutions from both DAS treatments exceeded the limit value recommended by the WHO. This justifies the incorporation of a polishing step following the DAS treatments (e.g., sulfate reduction or ultrafiltration) or the optimization of the BaCO₃-DAS to decrease the concentration of SO₄ contained in the final effluents.

These results indicate that the MgO-DAS treatment was more effective than the BaCO₃-DAS one for removing the divalent metals contained in the Parys Mountain AMD. The MgO-DAS technology allowed the near total elimination of dissolved metals in the pre-treated neutral AMD for an initial reactive mass:treated volume ratio of 1.2 g/L. The BaCO₃-DAS was also highly effective in eliminating the divalent metals (except for Mn), with a mass:volume ratio of 2.7 g/L. In addition, the latter treatment exhibited a higher effectiveness for eliminating sulfate from AMD.

3.3. Environmental and economic implications

Acidic waters emerging from the Dyffryn Adda adit at Parys Mountain constitute an important source of pollution to the Afon Goch Amlwch, which discharges into the Irish Sea (Mayes et al., 2010). This study proposes DAS technology as an effective and environmentally-friendly solution for the remediation of these acidic mine waters. Considering the total volume of AMD leachates that emerges from the Dyffryn Adda adit, i.e., around 378,000 m³/year, passive remediation using DAS technology could prevent the discharge of important amounts of contaminants into the Afon Goch Amlwch; e.g., around 153 tonnes/year Fe, 22 tonnes/year Al, 20 tonnes/year Zn, 12 tonnes/year Cu, 4 tonnes/year Mn, 137 kg/year As, 86 kg/year Co, 44 kg/year Cd, and 40 kg/year Ni. According to our estimates, around 739 tonnes of limestone and 454 tonnes of magnesia or 1021 tonnes of witherite would be needed to effectively treat the total annual volume of AMD discharged at Dyffryn Adda adit. Accounting for the market prices of limestone, magnesia, and witherite (around 13 USD/tonne, 250 USD/tonne, and 400 USD/tonne, respectively (https://www.alibaba.com; INAP, 2023)), the annual cost deriving from the purchase of these reagents would amount to around 123K USD for system 1 (limestone-DAS plus MgO-DAS) and 209K USD for system 2 (limestone-DAS plus BaCO₃-DAS).

The chemical precipitation of the dissolved metals in AMD during its treatment with passive DAS technology generates significant amounts of solid wastes. Thus, these solids could be considered a secondary source of base metals (i.e., Cu, Zn, Co, Ni, among others). In addition, other authors (e.g., Macías et al., 2017) have highlighted the high percentage of recovery of these metals using diluted acids (H₂SO₄ or HCl). Broad estimates of the potential value of metal reserves contained in the newly-formed solids during the alkaline treatment of AMD is shown in Table S4 in the supplementary material.

The prices of the metals published by the London Metal Exchange (LME) and the Shanghai Metals Market (SMM) (LME, 2023; SMM, 2023) were also consulted. Thus, a total economic value of around 309K USD/year was calculated for the metals contained in the wastes resulting from the DAS treatment. This value does not accommodate the processing, refining, or transport costs and is therefore overly optimistic. In this sense, technical limitations may limit the recovery of metals from these sludges and selective recovery methods should be developed to achieve a cost-effective recycling process (Macías et al., 2017; Chen et al., 2021). Smith et al. (2013) identified the need to apply a correction factor of 30% to obtain a figure closer to reality. After considering this correction factor, a total economic value of around 93K USD/year could be estimated for solid wastes resulting from the DAS treatment of AMD released from the Dyffryn Adda adit at Parys Mountain. Thus, the potential recovery of valuable metals from the DAS wastes could help to cover or offset costs associated with the treatment of these leachates. This approach is especially attractive for the mining and mineral processing industries, since the recycling of solid wastes from DAS treatments, as a source of base metals, would convert wastes into a marketable resource.

4. Conclusions

The main objective of this research work was to explore the efficiency of DAS technology for passive AMD treatments in areas characterized by a wet temperate oceanic climate. Combinations of several reactive columns filled with limestone-DAS, MgO-DAS, or BaCO₃-DAS mixtures were tested to select the best sequence of DAS treatment steps for effectively treating highly acidic and polluted AMD. The combination of two limestone-DAS sets followed by a MgO-DAS achieved average removal percentages of 100% for Fe, Al, Zn, Cu, Mn, As, and Co, and higher than 96% for Cd and Ni. This multistep treatment system was not effective for removing SO₄ (removal of around 7%). On the other hand, the combination of two limestone-DAS plus a BaCO₃-DAS showed a high effectiveness, reaching average elimination rates of 100% for Fe, Al, Cu and As, around 96% for Zn and Cd, and close to 81% for Co and Ni. Notably, this multistep treatment system was not as effective for Mn (removal of 63%). However, the system employing the BaCO₃-step showed a higher ability to remove SO₄ (around 53%) than the combined treatment with the MgO-step. According to PHREEQC calculations, the contaminant solubility in multistep DAS treatment systems could be controlled through the precipitation of oxy-hydroxy-sulfates (i.e., schwertmannite and basaluminite), carbonates (i.e., malachite, hydrozincite and calcite) and sulfate (i.e., barite).

The high efficiency achieved by the DAS technology was evidenced by the chemical compositions of the treated waters which had threshold values within irrigation standards, except for Mn in BaCO₃-DAS output waters. These results demonstrate that DAS technology is appropriate for the treatment of highly acidic and contaminated AMD from mining areas located in wet temperate oceanic climates. Thus, its use could drastically reduce the metallic contamination entering surrounding surface waterbodies and here the Irish Sea (around 153 tonnes/year Fe, 22 tonnes/year Al, 20 tonnes/year Zn, 12 tonnes/year Cu, 4 tonnes/year Mn, among others).

CRediT authorship contribution statement

Ricardo Millán-Becerro: Investigation, Data curation, Writing – original draft, Visualization. **Carlos R. Cánovas:** Investigation, Conceptualization, Writing – review & editing. **Francisco Macías:** Methodology, Conceptualization, Writing – review & editing. **Tobias S. Roetting:** Project administration, Writing – review & editing. **Louise Siddorn:** Writing – review & editing. **Peter Stanley:** Writing – review & editing. **Jose Miguel Nieto:** Project administration, Writing – review & editing.

Declaration of competing interest

The authors declare that they have no known competing financial interests or personal relationships that could have appeared to influence the work reported in this paper.

Data availability

Data will be made available on request.

Acknowledgements

Appendix A. Supplementary data

Supplementary data to this article can be found online at https://doi.org/10.1016/j.jclepro.2023.138872.

References

Akcil, A., Koldas, S., 2006. Acid Mine Drainage (AMD): causes, treatment and case studies. J. Clean. Prod. 14, 1139–1145. https://doi.org/10.1016/j.jclepro.2004.09.006.

Allison, J.D., Brown, D.S., Novo-Gradac, K.J., 1991. MINTEQA2/PRODEFA2, A Geochemical Assessment Model for Environmental Systems. Version 3.0 User's Manual, EPA/600/3-911021. Environmental Research Laboratory, Office of Research and Development, US Environmental Protection Agency, Athens, Georgia.

Ayers, R.S., Westcot, D.W., 1985. Water Quality for Agriculture, 29. Food and Agriculture Organization of the United Nations, Rome.

Ayora, C., Caraballo, M.A., Macías, F., Rötting, T.S., Carrera, J., Nieto, J.M., 2013. Acid mine drainage in the Iberian Pyrite Belt: 2. Lessons learned from recent passive remediation experiences. Environ. Sci. Pollut. Res. 20 (11), 7837–7853. https://doi.org/10.1007/s11356-013-1479-2.

Barrett, T.J., MacLean, W.J., Tennant, S.C., 2001. Volcanic sequence and alteration at the Parys Mountain volcanic-hosted massive sulfide deposit, Wales, United Kingdom: applications of immobile element lithogeochemistry. Econ. Geol. 96, 1279–1305. https://doi.org/10.2113/gsecongeo.96.5.1279.

Bevins, R.E., Young, B., Mason, J.S., Manning, D.A.C., Symes, R.F., 2010. Mineralization of england and Wales. Geological Conservation Review Series, No. 36 598. Joint Nature Conservation Committee, Peterborough.

Cánovas, C.R., Olías, M., Macias, F., Torres, E., San Miguel, E.G., Galván, L., Ayora, C., Nieto, J.M., 2016. Water acidification trends in a reservoir of the iberian pyrite Belt (SW Spain). Sci. Total Environ. 541, 400–411. https://doi.org/10.1016/j.scitotenv.2015.09.070.

Caraballo, M.A., Rötting, T.S., Nieto, J.M., Ayora, C., 2009. Sequential extraction and DXRD applicability to poorly crystalline Fe-and Al-phase characterization from an acid mine water passive remediation system. Am. Mineral. 94 (7), 1029–1038. https://doi.org/10.2138/am.2009.3137.

Caraballo, M.A., Rötting, T.S., Silva, V., 2010. Implementation of an MgO-based metal removal step in the passive treatment system of Shilbottle, UK: column experiments. J. Hazard Mater. 181 (1–3), 923–930. https://doi.org/10.1016/j.jhazmat.2010.05.100.

Caraballo, M.A., Macías, F., Nieto, J.M., Castillo, J., Quispe, D., Ayora, C., 2011a. Hydrochemical performance and mineralogical evolution of a dispersed alkaline substrate (DAS) remediating the highly polluted acid mine drainage in the full-scale passive treatment of Mina Esperanza (SW Spain). Am. Mineral. 96 (8–9), 1270–1277. https://doi.org/10.2138/am.2011.3752.

Caraballo, M.A., Macías, F., Rötting, T.S., Nieto, J.M., Ayora, C., 2011b. Long term remediation of highly polluted acid mine drainage: a sustainable approach to restore the environmental quality of the Odiel river basin. Environ. Pollut. 159 (12), 3613–3619. https://doi.org/10.1016/j.envpol.2011.08.003.

Chalkley, R., Child, F., Al-Thaqafi, K., Dean, A.P., White, K.N., Pittman, J.K., 2019. Macroalgae as spatial and temporal bioindicators of coastal metal pollution following remediation and diversion of acid mine drainage. Ecotoxicol. Environ. Saf. 182, 109458 https://doi.org/10.1016/j.ecoenv.2019.109458.

Chen, G., Ye, G., Yao, N., Hu, N., Zhang, J., Huang, Y., 2021. A critical review of prevention, treatment, reuse, and resource recovery from acid mine drainage. J. Clean. Prod. 329, 129666.

Cortina, J.L., Lagreca, I., De Pablo, J., Cama, J., Ayora, C., 2003. Passive in situ remediation of metal-polluted water with caustic magnesia: evidence from column experiments. Environ. Sci. Technol. 37, 1971–1977. https://doi.org/10.1021/es026018m.

Crane, R.A., Sinnett, D.E., Cleall, P.J., Sapsford, D.J., 2017. Physicochemical composition of wastes and co-located environmental designations at legacy mine sites in the south west of England and Wales: implications for their resource potential. Resour. Conserv. Recycl. 123, 117–134. https://doi.org/10.1016/j.resconrec.2016.08.009.

Dean, A.P., Lynch, S., Rowland, P., Toft, B.D., Pittman, J.K., White, K.N., 2013. Natural wetlands are efficient at providing long-term metal remediation of freshwater systems polluted by acid mine drainage. Environ. Sci. Technol. 47 (21), 12029–12036. https://doi.org/10.1021/es4025904.

DeGraff, J.V., 2007. Addressing the toxic legacy of abandoned mines on public land in the western United States. Rev. Eng. Geol. 17, 1–8. https://doi.org/10.1130/2007.4017(01.

Delgado, J., Barba-Brioso, C., Ayala, D., Boski, T., Torres, S., Calderón, E., López, F., 2019. Remediation experiment of Ecuadorian acid mine drainage: geochemical models of dissolved species and secondary minerals saturation. Environ. Sci. Pollut. Res. 26 (34), 34854–34872. https://doi.org/10.1007/s11356-019-06539-3.

Dewey, H., Smith, B., 1922. Lead and zinc ores in the pre-carboniferous rocks of west shropshire and north Wales, 23. Memoirs of the Geological Survey, Great Britain.

Ficklin, W.H., Plumlee, G.S., Smith, K.S., McHugh, J.B., 1992. Geochemical classification of mine drainages and natural drainages in mineralized areas. In: Proceedings of the 7th International Symposium on Water Rock Interaction, pp. 381–384 (Park City, Utah).

INAP (The International Network for Acid Prevention), 2023. Drainage treatment. http://www.gardguide.com/index.php?title=Chapter_7. (Accessed 15 January 2023).

Johnson, D.B., Hallberg, K.B., 2005. Acid mine drainage remediation options: a review. Sci. Total Environ. 338 (1–2), 3–14. https://doi.org/10.1016/j.scitotenv.2004.09.002.

Kirby, C.S., Cravotta, C.A., 2005. Net alkalinity and net acidity 1: theoretical considerations. Appl. Geochem. 20, 1920–1940. https://doi.org/10.1016/j.apgeochem.2005.07.002.

LME, 2023. London Metal Exchange Official Prices for Metal Global Market. https://lme.com/. (Accessed 10 January 2023).

Macías, F., Caraballo, M.A., Nieto, J.M., Rötting, T.S., Ayora, C., 2012a. Natural pretreatment and passive remediation of highly polluted acid mine drainage. J. Environ. Manag. 104, 93–100. https://doi.org/10.1016/j.jenvman.2012.03.027.

Macías, F., Caraballo, M.A., Rötting, T.S., Pérez-López, R., Nieto, J.M., Ayora, C., 2012b. From highly polluted Zn-rich acid mine drainage to non-metallic waters: implementation of a multi-step alkaline passive treatment system to remediate metal pollution. Sci. Total Environ. 433, 323–330. https://doi.org/10.1016/j.scitotenv.2012.06.084.

Macías, F., Pérez-López, R., Caraballo, M.A., Cánovas, C.R., Nieto, J.M., 2017. Management strategies and valorization for waste sludge from active treatment of extremely metal-polluted acid mine drainage: a contribution for sustainable mining. J. Clean. Prod. 141, 1057–1066. https://doi.org/10.1016/j.jclepro.2016.09.181.

Mayes, W.M., Potter, H.A.B., Jarvis, A.P., 2010. Inventory of aquatic contaminant flux arising from historical metal mining in England and Wales. Sci. Total Environ. 408, 3576–3583.

Nieto, J.M., Sarmiento, A.M., Canovas, C.R., Olias, M., Ayora, C., 2013. Acid mine drainage in the Iberian Pyrite Belt: 1. Hydrochemical characteristics and pollutant load of the Tinto and Odiel rivers. Environ. Sci. Pollut. Res. Int. 20 (11), 7509–7519. https://doi.org/10.1007/s11356-013-1634-9.

Nordstrom, D.K., 2009. Acid rock drainage and climate change. J. Geochem. Explor. 100, 97–104. https://doi.org/10.1016/j.gexplo.2008.08.002.

Nordstrom, D.K., 2011. Hydrogeochemical processes governing the origin, transport and fate of major and trace elements from mine wastes and mineralized rock to surface waters. Appl. Geochem. 26, 1777–1791. https://doi.org/10.1016/j.apgeochem.2011.06.002.

Nordstrom, D.K., Wilde, F.D., 1998. Reduction-oxidation potential (electrode method). In: National Field Manual for the Collection of Water Quality Data U.S. Geological Survey Techniques of Water-Resources Investigations, 9. Book (chapter 6.5).

Orden, S., Macías, F., Cánovas, C.R., Nieto, J.M., Pérez-López, R., Ayora, C., 2021. Eco-sustainable passive treatment for mine waters: full-scale and long-term demonstration. J. Environ. Manag. 280, 111699 https://doi.org/10.1016/j.jenvman.2020.111699.

Parkhurst, D.L., Appelo, C.A.J., 2005. PHREEQC-2 Version 2.12: a Hydrochemical Transport Model. http://wwwbrr.cr.usgs.gov2005.

Pérez-López, R., Macías, F., Caraballo, M.A., Nieto, J.M., Román-Ross, G., Tucoulou, R., Ayora, C., 2011. Mineralogy and geochemistry of Zn-rich mine-drainage precipitates from an MgO passive treatment system by synchrotron-based X-ray analysis. Environ. Sci. Technol. 45 (18), 7826–7833. https://doi.org/10.1021/es201667n.

Rakotonimaro, T.V., Neculita, C.M., Bussière, B., Zagury, G.J., 2016. Effectiveness of various dispersed alkaline substrates for the pre-treatment of ferriferous acid mine drainage. J. Appl. Geochem. 73, 13–23. https://doi.org/10.1016/j.apgeochem.2016.07.014.

Rakotonimaro, T.V., Neculita, C.M., Bussière, B., Genty, T., Zagury, G.J., 2018. Performance assessment of laboratory and field-scale multi-step passive treatment of iron-rich acid mine drainage for design improvement. Environ. Sci. Pollut. Res. 25 (18), 17575–17589. https://doi.org/10.1007/s11356-018-1820-x.

Ríos, C.A., Williams, C.D., Roberts, C.L., 2008. Removal of heavy metals from acid mine drainage (AMD) using coal fly ash, natural clinker and synthetic zeolites. J. Hazard Mater. 156, 23–35. https://doi.org/10.1016/j.jhazmat.2007.11.123.

Rötting, T.S., Cama, J., Ayora, C., Cortina, J.L., De Pablo, J., 2006a. Use of caustic magnesia to remove cadmium, nickel, and cobalt from water in passive treatment systems: column experiments. Environ. Sci. Technol. 40 (20), 6438–6443. https://doi.org/10.1021/es061092g.

Rötting, T.S., Thomas, R.C., Ayora, C., Carrera, J., 2006b. Challenges of passive treatment of metal mine drainage in the Iberian Pyrite Belt (Southern Spain): preliminary studies. In: Proc. Of the Seventh Int. Conf. On Acid Rock Drainage, St. Louis, MO, pp. 1753–1767.

Rowlands, J., 1981. Copper Mountain. Anglesey Antiquarian Society.

Sánchez-España, J., Yusta, I., Diez-Ercilla, M., 2011. Schwertmannite and hydrobasaluminite: a re-evaluation of their solubility and control on the iron and aluminium concentration in acidic pit lakes. J. Appl. Geochem. 26 (9–10), 1752–1774. https://doi.org/10.1016/j.apgeochem.2011.06.020.

Sarmiento, A.M., Nieto, J.M., Olías, M., Cánovas, C.R., 2009. Hydrochemical characteristics and seasonal influence on the pollution by acid mine drainage in the Odiel river Basin (SW Spain). J. Appl. Geochem. 24 (4), 697–714. https://doi.org/10.1016/j.apgeochem.2008.12.025.

Schindler, P., Reinert, M., Gamsjager, H., 1969. Thermodynamics of metal carbonates3. Solubility constants and free formation enthalpies of $ZnCO_3$ and $Zn_5(OH)_6(CO_3)_2$ at 25 degrees. Helv. Chim. Acta 52 (8), 2327–2332.

Smith, K.L., Figueroa, L.A., Plumlee, G.S., 2013. Can treatment and disposal costs be reduced through metal recovery? In: Wolkersdorfer, Brown, Figueroa (Eds.), Proceedings of the Annual International Mine Water Association Conference-Reliable Mine Water Technology. Golden, Colorado (USA).

SMM, 2023. Shangai Metals Market. https://www.metal.com/. (Accessed 10 January 2023).

Torres, E., Lozano, A., Macías, F., Gomez-Arias, A., Castillo, J., Ayora, C., 2018. Passive elimination of sulfate and metals from acid mine drainage using combined limestone and barium carbonate systems. J. Clean. Prod. 182, 114–123. https://doi.org/10.1016/j.jclepro.2018.01.224.

Tripole, S., Gonzalez, P., Vallania, A., Garbagnati, M., Mallea, M., 2006. Evaluation of the impact of acid mine drainage on the chemistry and the macrobenthos in the Carolina Stream (San Luis-Argentina). Environ. Monit. Assess. 114, 377–389. https://doi.org/10.1007/s10661-006-4941-5.

WHO, 2011. Guidelines for Drinking-Water Quality, fourth ed. World Health Organization. http://www.who.int/water_sanitation_health/publications/2011/dwq_guidelines/en/index.html. (Accessed 27 January 2023).

Younger, P.L., 1997. The longevity of minewater pollution: a basis for decision-making. Sci. Total Environ. 194, 457–466. https://doi.org/10.1016/S0048-9697(96)05383-1. –195.

Younger, P.L., Potter, H.A.B., 2012. Parys in springtime: hazard management and steps towards remediation of the UK's most polluted acidic mine discharge. In: 9th International Conference on Acid Rock Drainage (ICARD), Ottawa, Canada.